2018 26th Mediterranean Conference on Control and Automation (MED)
Zadar, Croatia, June 19-22, 2018

Robust time-varying sensor bias estimation for bounded-error systems: Application to the wind turbine benchmark

Marcin Witczak[1], Marcin Pazera[1], Vicenç Puig[2] and Marcin Mrugalski[1]

Abstract— **The objective of this paper is to propose a novel approach for simultaneous state and time-varying sensor bias estimation of dynamic systems. The main advantage of the presented strategy is its simplicity along with robustness to exogenous bounded disturbances. The proposed approach belongs to the wide class of the so-called bounded-error approaches. It constitutes an attractive alternative to the stochastic Kalman-filer-based framework as no knowledge about disturbances/noise distribution is required. The only preliminary requirement is the knowledge about their upper and lower bounds. In this paper, it is assumed that their belong the the ellipsoidal set. Under such an assumption, a novel estimator is proposed along with a comprehensive convergence analysis. It is worth to note that, the convergence analysis is realised with the so-called quadratic boundedness approach. The final part of the paper concerns application of the proposed approach to the wind turbine benchmark.**

I. INTRODUCTION

The problem of simultaneous state and sensor bias estimation has received a significant attention in the literature. Its importance is clearly justified by a large number of applications such control and health monitoring. A traditional way to settle it is to use a bank of observers. Each observer is using all but one sensors and estimates the missing sensor readings. These estimates are then compared with real sensor measurements and, as a result, the sensor bias is obtained. An obvious drawback of such a scheme is that it is assumed that, within a given time interval, only one sensor readings are impaired by bias. There are of course plenty of more efficient approaches and some of them are listed below. In [6], [7], the multiple sensor bias estimation based on the so-called local tracks is proposed. The estimation of constant and dynamic biases in asynchronous multi-sensor systems based on the measurements from asynchronous sensors into pseudo-measurements of the sensor biases is presented in [12]. A linear time-varying approach for simultaneous estimation of a linear velocity and acceleration constant bias of a quad-rotor is proposed in [13] while in [17] an $\mathcal{H}_\infty$ approach along with a linear parameter-varying approach are taken into account to estimate the yaw rate sensor bias for an electric vehicle. A joint estimation of sensor biases and unknown point of interest location using multiple unmanned aerial vehicles is proposed in [16]. An adaptive technique to the estimation of an unknown sensor bias for a class of nonlinear discrete-time systems is proposed in [15]. A bank of isolation estimators, each corresponding to a particular output sensor is presented in [18]. An adaptive Kalman-filter-based technique to estimate and remove sensor biases in a multiradar system is investigated in [3]. An $\mathcal{H}_\infty$ approach is proposed in [11] for designing a sensor fault estimator and fault-tolerant controller as well. Indeed, some of the fault-tolerant approaches are applied in many potential applications [14]. Finally, a scheme based on the design of nonlinear observers for unknown bias identification and state estimation is used in fault-tolerant control application of a spacecraft [2].

The paper introduces a novel approach for simultaneous state and time-varying sensor bias estimation of uncertain linear systems. The proposed strategy is based on a single observer only and its main advantage boils down to its simplicity along with robustness to exogenous bounded disturbances. It constitutes an attractive alternative to the stochastic Kalman-filer-based framework as no knowledge about disturbances/noise distribution is required. The only preliminary assumption is related to the knowledge about their upper and lower bounds.

The paper is organized as follows. Section II portrays preliminary assumptions. In Section III, the structure of a new estimator is proposed along with a comprehensive convergence analysis. Section IV presents the results concerning the application of the proposed approach to the wind-turbine benchmark [9], [8]. Finally, the last section concludes the paper.

II. PRELIMINARIES

Let us consider the following discrete-time system:

$$\boldsymbol{x}_{k+1} = \boldsymbol{A}\boldsymbol{x}_k + \boldsymbol{B}\boldsymbol{u}_k + \boldsymbol{W}_1\boldsymbol{w}_k, \tag{1}$$

$$\boldsymbol{y}_k = \boldsymbol{C}\boldsymbol{x}_k + \boldsymbol{f}_{s,k} + \boldsymbol{W}_2\boldsymbol{w}_k, \tag{2}$$

where $\boldsymbol{x}_k \in \mathbb{X} \subset \mathbb{R}^n$ is the state vector, $\boldsymbol{u}_k \in \mathbb{R}^r$ stands for the control input, $\boldsymbol{y}_k \in \mathbb{R}^m$ is the output. Moreover, $\boldsymbol{f}_{s,k} \in \mathbb{F}_s \subset \mathbb{R}^m$ is an unknown sensor bias vector and $\boldsymbol{w}_k \in \mathbb{R}^s$ expresses an exogenous disturbance. It can be easily shown that it can be split in such a way as $\boldsymbol{w}_k = \left[\boldsymbol{w}_{1,k}^T, \boldsymbol{w}_{2,k}^T\right]^T$, where each component represents the process and measurement uncertainties, respectively. Moreover, let the exogenous disturbance vector satisfy the following assumption:

Assumption 1:

$$\boldsymbol{w}_k \in \mathbb{E}_w = \{\boldsymbol{w} : \boldsymbol{w}^T\boldsymbol{Q}_w\boldsymbol{w} \leq 1\}, \quad \boldsymbol{Q}_w \succ 0. \tag{3}$$

This assumption states that the external disturbances are unknown but bounded. The general idea that states behind

[1]Institute of Control and Computation Engineering, University of Zielona Góra, ul. Podgórna 50, 65-246 Zielona Góra, Poland, {M.Witczak,M.Pazera,M.Mrugalski}@issi.uz.zgora.pl
[2]Automatic Control Department, Universitat Politécnica de Catalunya (UPC), Rambla de Sant Nebridi, 11, 08222 Terrassa, vicenc.puig@upc.edu

978-1-5386-7891-6/18/$31.00 ©2018 IEEE

this approach is that it provides knowledge about the lower and upper bounds of the external disturbances in the form of an ellipsoid.

III. Fault estimator design

The main objective of this section is to propose the estimator structure, which will be able to estimate the state and, as a consequence, the sensor bias. By extracting the sensor bias from (2), it can be easily shown that

$$\boldsymbol{f}_{s,k} = \boldsymbol{y}_k - \boldsymbol{C}\boldsymbol{x}_k - \boldsymbol{W}_2\boldsymbol{w}_k. \tag{4}$$

In this point, a simple bias estimator, which resembles (4), is proposed

$$\hat{\boldsymbol{f}}_{s,k} = \boldsymbol{y}_k - \boldsymbol{C}\boldsymbol{A}\hat{\boldsymbol{x}}_{k-1} - \boldsymbol{C}\boldsymbol{B}\boldsymbol{u}_{k-1}. \tag{5}$$

Subsequently, using (1)–(2), equation (5) can be expressed as

$$\hat{\boldsymbol{f}}_{s,k} = \boldsymbol{f}_{s,k} + \boldsymbol{C}\boldsymbol{A}\boldsymbol{e}_{k-1} + \boldsymbol{C}\boldsymbol{W}_1\boldsymbol{w}_{k-1} + \boldsymbol{W}_2\boldsymbol{w}_k, \tag{6}$$

where

$$\boldsymbol{e}_k = \boldsymbol{x}_k - \hat{\boldsymbol{x}}_k, \tag{7}$$

is the state estimation error. Having the bias estimator (6), it is possible to propose the state estimator of the form

$$\hat{\boldsymbol{x}}_{k+1} = \boldsymbol{A}\hat{\boldsymbol{x}}_k + \boldsymbol{B}\boldsymbol{u}_k + \boldsymbol{K}\left(\boldsymbol{y}_k - \boldsymbol{C}\hat{\boldsymbol{x}}_k - \hat{\boldsymbol{f}}_{s,k}\right). \tag{8}$$

Substituting (2) and (6) into (8) yields

$$\begin{aligned}\hat{\boldsymbol{x}}_{k+1} = {} & \boldsymbol{A}\hat{\boldsymbol{x}}_k + \boldsymbol{B}\boldsymbol{u}_k + \boldsymbol{K}\boldsymbol{C}\boldsymbol{e}_k - \boldsymbol{K}\boldsymbol{C}\boldsymbol{A}\boldsymbol{e}_{k-1} \\ & - \boldsymbol{K}\boldsymbol{C}\boldsymbol{W}_1\boldsymbol{w}_{k-1}.\end{aligned} \tag{9}$$

Thus, bearing in mind (1)–(2) as well as (9), the dynamics of the state estimation error can be described as follows

$$\begin{aligned}\boldsymbol{e}_{k+1} = {} & \boldsymbol{x}_{k+1} - \hat{\boldsymbol{x}}_{k+1} = \boldsymbol{A}\boldsymbol{x}_k + \boldsymbol{B}\boldsymbol{u}_k + \boldsymbol{W}_1\boldsymbol{w}_k \\ & - \boldsymbol{A}\hat{\boldsymbol{x}}_k - \boldsymbol{B}\boldsymbol{u}_k - \boldsymbol{K}\boldsymbol{C}\boldsymbol{e}_k - \boldsymbol{K}\boldsymbol{C}\boldsymbol{A}\boldsymbol{e}_{k-1} \\ & - \boldsymbol{K}\boldsymbol{C}\boldsymbol{W}_1\boldsymbol{w}_{k-1} = [\boldsymbol{A} - \boldsymbol{K}\boldsymbol{C}]\,\boldsymbol{e}_k \\ & + \boldsymbol{K}\boldsymbol{C}\boldsymbol{A}\boldsymbol{e}_{k-1} + \boldsymbol{W}_1\boldsymbol{w}_k - \boldsymbol{K}\boldsymbol{C}\boldsymbol{W}_1\boldsymbol{w}_{k-1}.\end{aligned} \tag{10}$$

In a similar fashion, the sensor bias estimation error can be described by

$$\begin{aligned}\boldsymbol{e}_{s,k} = {} & \boldsymbol{f}_{s,k} - \hat{\boldsymbol{f}}_{s,k} = -\boldsymbol{C}\boldsymbol{A}\boldsymbol{e}_{k-1} - \boldsymbol{W}_2\boldsymbol{w}_k \\ & - \boldsymbol{C}\boldsymbol{W}_1\boldsymbol{w}_{k-1}.\end{aligned} \tag{11}$$

Note that, both the state estimation error $\boldsymbol{e}_{k+1}$ and the bias estimation error $\boldsymbol{e}_{s,k}$ depend only on the state estimation error $\boldsymbol{e}_k$ and exogenous disturbances $\boldsymbol{w}_k$. This means that the design procedure boils down to designing $\boldsymbol{K}$ only.

It can be shown that the state estimation error can be rewritten into the following compact form

$$\boldsymbol{e}_{k+1} = \boldsymbol{A}_1\boldsymbol{e}_k + \boldsymbol{A}_2\boldsymbol{e}_{k-1} + \boldsymbol{W}_1\boldsymbol{w}_k + \boldsymbol{W}_3\boldsymbol{w}_{k-1}, \tag{12}$$

where

$$\boldsymbol{A}_1 = \boldsymbol{A} - \boldsymbol{K}\boldsymbol{C}, \tag{13}$$

$$\boldsymbol{A}_2 = \boldsymbol{K}\boldsymbol{C}\boldsymbol{A}, \tag{14}$$

$$\boldsymbol{W}_3 = \boldsymbol{K}\boldsymbol{C}\boldsymbol{W}_1. \tag{15}$$

For the purpose of further analysis, it is proposed to use the so-called Quadratic Boundedness (QB) [1], [5], [4] approach. Originally, such a methodology was used to design a state estimator for linear uncertain discrete time systems. However, the extension proposed in this paper allows obtaining the estimator which is able to estimate the state and sensor bias as well. Let us formulate the Lyapunov candidate function

$$V_k = \boldsymbol{e}_k^T\boldsymbol{P}\boldsymbol{e}_k + \boldsymbol{e}_{k-1}^T\boldsymbol{R}\boldsymbol{e}_{k-1}, \tag{16}$$

with $\boldsymbol{P} \succ 0$ and $\boldsymbol{R} \succ 0$.

To introduce the QB approach [1], [5], [4], let us remind the following definitions:

Definition 1: The system (12) is strictly quadratically bounded for all allowable $\boldsymbol{w}_k \in \mathbb{E}_w$, if $\boldsymbol{e}_k^T\boldsymbol{P}\boldsymbol{e}_k > 1$ implies $\boldsymbol{e}_{k+1}^T\boldsymbol{P}\boldsymbol{e}_{k+1} < \boldsymbol{e}_k^T\boldsymbol{P}\boldsymbol{e}_k$ for any $\boldsymbol{w}_k \in \mathbb{E}_w$.

Note that the strict quadratic boundedness of (12) ensures that $V_{k+1} < V_k$ for any $\boldsymbol{w}_k \in \mathbb{E}_w$ when $V_k > 1$.

Definition 2: A set $\mathbb{E}$ is a positively invariant set for (12) for all $\boldsymbol{w}_k \in \mathbb{E}_w$ if $\boldsymbol{e}_k \in \mathbb{E}$ implies $\boldsymbol{e}_{k+1} \in \mathbb{E}$ for any $\boldsymbol{w}_k \in \mathbb{E}_w$.

Note that if $\boldsymbol{e}_k$ is outside an invariant set $\mathbb{E}$, i.e., $V_k > 1$, then V_k decreases until $\boldsymbol{e}_k$ comes back to the invariant set $\mathbb{E}$. This means that the proposed scheme provides knowledge about lower and upper bounds of the system states that can be perceived as worst-case situations.

Based on the aforementioned definitions and results presented in [1], the following lemma is proposed for (12):

Lemma 1: The following statements are equivalent:

1) The system (12) is strictly quadratically bounded for all $\boldsymbol{w}_k \in \mathbb{E}_w$,
2) The ellipsoid

$$\mathbb{E} = \{\boldsymbol{e}_k : \begin{bmatrix}\boldsymbol{e}_k \\ \boldsymbol{e}_{k-1}\end{bmatrix}^T \begin{bmatrix}\boldsymbol{P} & \boldsymbol{0} \\ \boldsymbol{0} & \boldsymbol{R}\end{bmatrix} \begin{bmatrix}\boldsymbol{e}_k \\ \boldsymbol{e}_{k-1}\end{bmatrix} \le 1\}, \tag{17}$$

is a robust invariant set for (12) for any $\boldsymbol{w}_k \in \mathbb{E}_w$,
3) There exist a scalar $\alpha \in (0,1)$ such that

$$\begin{bmatrix} \boldsymbol{X}^T\boldsymbol{P}\boldsymbol{X} + \boldsymbol{R} - \boldsymbol{P} + \alpha\boldsymbol{P} & \boldsymbol{X}^T\boldsymbol{P}\boldsymbol{Z} & \boldsymbol{X}^T\boldsymbol{P}\boldsymbol{W} & \boldsymbol{X}^T\boldsymbol{P}\boldsymbol{Y} \\ \boldsymbol{Z}^T\boldsymbol{P}\boldsymbol{X} & \boldsymbol{Z}^T\boldsymbol{P}\boldsymbol{Z} - \boldsymbol{R} + \alpha\boldsymbol{R} & \boldsymbol{Z}^T\boldsymbol{P}\boldsymbol{W} & \boldsymbol{Z}^T\boldsymbol{P}\boldsymbol{Y} \\ \boldsymbol{W}^T\boldsymbol{P}\boldsymbol{X} & \boldsymbol{W}^T\boldsymbol{P}\boldsymbol{Z} & \boldsymbol{W}^T\boldsymbol{P}\boldsymbol{W} - \alpha\boldsymbol{Q}_w & \boldsymbol{W}^T\boldsymbol{P}\boldsymbol{Y} \\ \boldsymbol{Y}^T\boldsymbol{P}\boldsymbol{X} & \boldsymbol{Y}^T\boldsymbol{P}\boldsymbol{Z} & \boldsymbol{Y}^T\boldsymbol{P}\boldsymbol{W} & \boldsymbol{Y}^T\boldsymbol{P}\boldsymbol{Y} - \alpha\boldsymbol{Q}_w \end{bmatrix} \prec 0, \tag{18}$$

The subsequent theorem constitutes the main result of the paper:

Theorem 1: The system (12) is strictly quadratically bounded for all $\boldsymbol{w}_k \in \mathbb{E}_w$ if there exist matrices $\boldsymbol{P} \succ 0$, $\boldsymbol{U}$, $\boldsymbol{R} \succ 0$ and a scalar $\alpha \in (0,1)$, such that the following inequality is satisfied

$$\begin{bmatrix} \boldsymbol{R}-\boldsymbol{P}+\alpha\boldsymbol{P} & \boldsymbol{0} & \boldsymbol{0} & \boldsymbol{0} & \boldsymbol{A}^T\boldsymbol{P}-\boldsymbol{C}^T\boldsymbol{U}^T \\ \boldsymbol{0} & -\boldsymbol{R}+\alpha\boldsymbol{R} & \boldsymbol{0} & \boldsymbol{0} & \boldsymbol{A}^T\boldsymbol{C}^T\boldsymbol{U}^T \\ \boldsymbol{0} & \boldsymbol{0} & -\alpha\boldsymbol{Q}_w & \boldsymbol{0} & \boldsymbol{W}_1^T\boldsymbol{P} \\ \boldsymbol{0} & \boldsymbol{0} & \boldsymbol{0} & -\alpha\boldsymbol{Q}_w & \boldsymbol{W}_1^T\boldsymbol{C}^T\boldsymbol{U}^T \\ \boldsymbol{P}\boldsymbol{A}-\boldsymbol{U}\boldsymbol{C} & \boldsymbol{U}\boldsymbol{C}\boldsymbol{A} & \boldsymbol{P}\boldsymbol{W}_1 & \boldsymbol{U}\boldsymbol{C}\boldsymbol{W}_1 & -\boldsymbol{P} \end{bmatrix} \prec 0. \tag{19}$$

Proof: Based on (16) and (18) it can be observed that QB is equivalent to

$$\begin{aligned} &V_{k+1}-(1-\alpha)V_k-\alpha\boldsymbol{w}_k^T\boldsymbol{Q}_w\boldsymbol{w}_k \\ &\quad -\alpha\boldsymbol{w}_{k-1}^T\boldsymbol{Q}_w\boldsymbol{w}_{k-1}<0, \end{aligned} \tag{20}$$

which leads to

$$\begin{aligned} &\boldsymbol{e}_{k+1}^T\boldsymbol{P}\boldsymbol{e}_{k+1}+\boldsymbol{e}_k^T(\boldsymbol{R}-\boldsymbol{P})\boldsymbol{e}_k+\alpha\boldsymbol{e}_k^T\boldsymbol{P}\boldsymbol{e}_k \\ &\quad +\alpha\boldsymbol{e}_{k-1}^T\boldsymbol{R}\boldsymbol{e}_{k-1}-\boldsymbol{e}_{k-1}^T\boldsymbol{R}\boldsymbol{e}_{k-1} \\ &\quad -\alpha\boldsymbol{w}_k^T\boldsymbol{Q}_w\boldsymbol{w}_k \\ &\quad -\alpha\boldsymbol{w}_{k-1}^T\boldsymbol{Q}_w\boldsymbol{w}_{k-1}<0. \end{aligned} \tag{21}$$

Using (12) it can be shown that

$$\begin{aligned} &V_{k+1}-(1-\alpha)V_k-\alpha\boldsymbol{w}_k^T\boldsymbol{Q}_w\boldsymbol{w}_k-\alpha\boldsymbol{w}_{k-1}^T\boldsymbol{Q}_w\boldsymbol{w}_{k-1} \\ &\quad =\boldsymbol{e}_k^T\left(\boldsymbol{A}_1^T\boldsymbol{P}\boldsymbol{A}_1+\boldsymbol{R}-\boldsymbol{P}+\alpha\boldsymbol{P}\right)\boldsymbol{e}_k \\ &\quad +\boldsymbol{e}_k^T\left(\boldsymbol{A}_1^T\boldsymbol{P}\boldsymbol{A}_2\right)\boldsymbol{e}_{k-1}+\boldsymbol{e}_k^T\left(\boldsymbol{A}_1^T\boldsymbol{P}\boldsymbol{W}_1\right)\boldsymbol{w}_k \\ &\quad +\boldsymbol{e}_k^T\left(\boldsymbol{A}_1^T\boldsymbol{P}\boldsymbol{W}_3\right)\boldsymbol{w}_{k-1}+\boldsymbol{e}_{k-1}^T\left(\boldsymbol{A}_2^T\boldsymbol{P}\boldsymbol{A}_1\right)\boldsymbol{e}_k \\ &\quad +\boldsymbol{e}_{k-1}^T\left(\boldsymbol{A}_2^T\boldsymbol{P}\boldsymbol{A}_2-\boldsymbol{R}+\alpha\boldsymbol{R}\right)\boldsymbol{e}_{k-1} \\ &\quad +\boldsymbol{e}_{k-1}^T\left(\boldsymbol{A}_2^T\boldsymbol{P}\boldsymbol{W}_1\right)\boldsymbol{w}_k+\boldsymbol{e}_{k-1}^T\left(\boldsymbol{A}_2^T\boldsymbol{P}\boldsymbol{W}_3\right)\boldsymbol{w}_{k-1} \\ &\quad +\boldsymbol{w}_k^T\left(\boldsymbol{W}_1^T\boldsymbol{P}\boldsymbol{A}_1\right)\boldsymbol{e}_k+\boldsymbol{w}_k^T\left(\boldsymbol{W}_1^T\boldsymbol{P}\boldsymbol{A}_2\right)\boldsymbol{e}_{k-1} \\ &\quad +\boldsymbol{w}_k^T\left(\boldsymbol{W}_1^T\boldsymbol{P}\boldsymbol{W}_1-\alpha\boldsymbol{Q}_w\right)\boldsymbol{w}_k \\ &\quad +\boldsymbol{w}_k^T\left(\boldsymbol{W}_1^T\boldsymbol{P}\boldsymbol{W}_3\right)\boldsymbol{w}_{k-1}+\boldsymbol{w}_{k-1}^T\left(\boldsymbol{W}_3^T\boldsymbol{P}\boldsymbol{A}_1\right)\boldsymbol{e}_k \\ &\quad +\boldsymbol{w}_{k-1}^T\left(\boldsymbol{W}_3^T\boldsymbol{P}\boldsymbol{A}_2\right)\boldsymbol{e}_{k-1}+\boldsymbol{w}_{k-1}^T\left(\boldsymbol{W}_3^T\boldsymbol{P}\boldsymbol{W}_1\right)\boldsymbol{w}_k \\ &\quad +\boldsymbol{w}_{k-1}^T\left(\boldsymbol{W}_3^T\boldsymbol{P}\boldsymbol{W}_3-\alpha\boldsymbol{Q}_w\right)\boldsymbol{w}_{k-1}<0. \end{aligned} \tag{22}$$

By introducing

$$\bar{\boldsymbol{v}}_k=\begin{bmatrix}\boldsymbol{e}_k^T & \boldsymbol{e}_{k-1}^T & \boldsymbol{w}_k^T & \boldsymbol{w}_{k-1}^T\end{bmatrix}^T, \tag{23}$$

inequality (22) can be rewritten into the following form

$$\bar{\boldsymbol{v}}_k^T\begin{bmatrix} \boldsymbol{A}_1^T\boldsymbol{P}\boldsymbol{A}_1+\boldsymbol{R}-\boldsymbol{P}+\alpha\boldsymbol{P} & \boldsymbol{A}_1^T\boldsymbol{P}\boldsymbol{A}_2 & \boldsymbol{A}_1^T\boldsymbol{P}\boldsymbol{W}_1 & \boldsymbol{A}_1^T\boldsymbol{P}\boldsymbol{W}_3 \\ \boldsymbol{A}_2^T\boldsymbol{P}\boldsymbol{A}_1 & \boldsymbol{A}_2^T\boldsymbol{P}\boldsymbol{A}_2-\boldsymbol{R}+\alpha\boldsymbol{R} & \boldsymbol{A}_2^T\boldsymbol{P}\boldsymbol{W}_1 & \boldsymbol{A}_2^T\boldsymbol{P}\boldsymbol{W}_3 \\ \boldsymbol{W}_1^T\boldsymbol{P}\boldsymbol{A}_1 & \boldsymbol{W}_1^T\boldsymbol{P}\boldsymbol{A}_2 & \boldsymbol{W}_1^T\boldsymbol{P}\boldsymbol{W}_1-\alpha\boldsymbol{Q}_w & \boldsymbol{W}_1^T\boldsymbol{P}\boldsymbol{W}_3 \\ \boldsymbol{W}_3^T\boldsymbol{P}\boldsymbol{A}_1 & \boldsymbol{W}_3^T\boldsymbol{P}\boldsymbol{A}_2 & \boldsymbol{W}_3^T\boldsymbol{P}\boldsymbol{W}_1 & \boldsymbol{W}_3^T\boldsymbol{P}\boldsymbol{W}_3-\alpha\boldsymbol{Q}_w \end{bmatrix}\bar{\boldsymbol{v}}_k \prec 0, \tag{24}$$

or alternatively

$$\begin{bmatrix}\boldsymbol{A}_1^T \\ \boldsymbol{A}_2^T \\ \boldsymbol{W}_1^T \\ \boldsymbol{W}_3^T\end{bmatrix}\boldsymbol{P}\begin{bmatrix}\boldsymbol{A}_1 & \boldsymbol{A}_2 & \boldsymbol{W}_1 & \boldsymbol{W}_3\end{bmatrix} + \begin{bmatrix} \boldsymbol{R}-\boldsymbol{P}+\alpha\boldsymbol{P} & \boldsymbol{0} & \boldsymbol{0} & \boldsymbol{0} \\ \boldsymbol{0} & -\boldsymbol{R}+\alpha\boldsymbol{R} & \boldsymbol{0} & \boldsymbol{0} \\ \boldsymbol{0} & \boldsymbol{0} & -\alpha\boldsymbol{Q}_w & \boldsymbol{0} \\ \boldsymbol{0} & \boldsymbol{0} & \boldsymbol{0} & -\alpha\boldsymbol{Q}_w \end{bmatrix} \prec 0. \tag{25}$$

Then using Schur complements and multiplying from left and right side by diag $(\boldsymbol{I},\boldsymbol{I},\boldsymbol{I},\boldsymbol{I},\boldsymbol{P})$ give

$$\begin{bmatrix} \boldsymbol{R}-\boldsymbol{P}+\alpha\boldsymbol{P} & \boldsymbol{0} & \boldsymbol{0} & \boldsymbol{0} & \boldsymbol{A}_1^T\boldsymbol{P} \\ \boldsymbol{0} & -\boldsymbol{R}+\alpha\boldsymbol{R} & \boldsymbol{0} & \boldsymbol{0} & \boldsymbol{A}_2^T\boldsymbol{P} \\ \boldsymbol{0} & \boldsymbol{0} & -\alpha\boldsymbol{Q}_w & \boldsymbol{0} & \boldsymbol{W}_1^T\boldsymbol{P} \\ \boldsymbol{0} & \boldsymbol{0} & \boldsymbol{0} & -\alpha\boldsymbol{Q}_w & \boldsymbol{W}_3^T\boldsymbol{P} \\ \boldsymbol{P}\boldsymbol{A}_1 & \boldsymbol{P}\boldsymbol{A}_2 & \boldsymbol{P}\boldsymbol{W}_1 & \boldsymbol{P}\boldsymbol{W}_3 & -\boldsymbol{P} \end{bmatrix} \prec 0. \tag{26}$$

Introducing

$$\begin{aligned} \boldsymbol{P}\boldsymbol{A}_1 &= \boldsymbol{P}(\boldsymbol{A}-\boldsymbol{K}\boldsymbol{C})=\boldsymbol{P}\boldsymbol{A}-\boldsymbol{P}\boldsymbol{K}\boldsymbol{C} \\ &= \boldsymbol{P}\boldsymbol{A}-\boldsymbol{U}\boldsymbol{C}, \end{aligned} \tag{27}$$

$$\boldsymbol{P}\boldsymbol{A}_2=\boldsymbol{P}\boldsymbol{K}\boldsymbol{C}\boldsymbol{A}=\boldsymbol{U}\boldsymbol{C}\boldsymbol{A}, \tag{28}$$

$$\boldsymbol{P}\boldsymbol{W}_3=\boldsymbol{P}\boldsymbol{K}\boldsymbol{C}\boldsymbol{W}_1=\boldsymbol{U}\boldsymbol{C}\boldsymbol{W}_1, \tag{29}$$

and applying (27)–(29) to (26) completes the proof. ■

Finally, the design procedure boils down to solve (19) and then calculate

$$\boldsymbol{K}=\boldsymbol{P}^{-1}\boldsymbol{U}. \tag{30}$$

Note that, the problem of solving (19) boils down to bilinear matrix inequalities, due to the products of $\alpha\boldsymbol{P}$ and $\alpha\boldsymbol{R}$. However, fixing the value of α, (19) becomes a set of LMIs. Since α is constrained by the interval $(0,1)$, an iterative algorithm can be easily implemented.

The main goal of the next section is to show the effectiveness and performance of the proposed approach.

IV. ILLUSTRATIVE EXAMPLE

In order to confirm the correctness and performances of the proposed strategy, its implementation to the wind turbine benchmark [9], [8] was performed. This is a three-blade horizontal-axis, pitch controlled, variable speed turbine. The results in this paper are limited to the drive train and hydraulic pitch subsystems of the wind turbine. For the purpose of estimation of the state and sensor biases, the pitch and drive train subsystems can be considered independently and for such a reason two separate estimators were designed.

The drive train [10] of the wind turbine may be modelled by following equations:

$$\dot{\omega}_r(t) = -\frac{B_{dt}+B_r}{J_r}\omega_r(t) + \frac{B_{dt}}{N_g J_r}\omega_g(t) - \frac{K_{dt}}{J_r}\theta_\Delta(t) + \frac{T_r(t)}{J_r}, \tag{31}$$

$$\dot{\omega}_g(t) = \frac{\eta_{dt}B_{dt}}{N_g J_g}\omega_r(t) - \left(\frac{\eta_{dt}B_{dt}}{N_g^2 J_g} + \frac{B_g}{J_g}\right)\omega_g(t) + \frac{\eta_{dt}K_{dt}}{N_g J_g}\theta_\Delta(t) - \frac{T_g(t)}{J_g}, \tag{32}$$

$$\dot{\theta}_\Delta(t) = \omega_r(t) - \frac{\omega_g(t)}{N_g}, \tag{33}$$

where ω_r, ω_g, θ_Δ are the rotor speed, generator speed and torsion angle, respectively. Whereas the hydraulic pitch subsystem [10] may be modelled as a second-order system

$$\ddot{\beta}_i(t) = -2\zeta_i\omega_g n, i\dot{\beta}_i(t) + \omega_{n,i}^2\beta_{i,ref}(t), \tag{34}$$

where β_i is the pitch angle of the ith blade, with $i = 1, 2, 3$. All of the parameters were inherited from [8] and are presented in Table I. The above equations which are

TABLE I
VALUES OF THE PARAMETERS

Parameter	Value
B_{dt}	775.49
B_r	7.11
J_r	$55 \cdot 10^6$
N_g	95
K_{dt}	$2.7 \cdot 10^9$
η_{dt}	0.97
J_g	390
$B_{g,0}$	45.6
$\omega_{n,0}$	11.11
ζ_0	0.6

describing the behaviour of the system were discretized using Euler method with sampling time $T_s = 0.01[s]$. The following state-space, discrete-time system for the drive train was obtained:

$$\boldsymbol{A}_{dt} = \begin{bmatrix} 1.0000 & 0.0000 & -0.0005 \\ 0.0002 & 0.9988 & 0.0191 \\ 0.0100 & -0.0001 & 0.9900 \end{bmatrix}, \tag{35}$$

$$\boldsymbol{B}_{dt} = 10^{-4} \cdot \begin{bmatrix} 0.0000 & 0 \\ 0 & -0.2564 \\ 0 & 0 \end{bmatrix}, \tag{36}$$

$$\boldsymbol{C}_{dt} = \begin{bmatrix} 1 & 0 & 0 \\ 0 & 1 & 0 \end{bmatrix}. \tag{37}$$

In the same fashion, using the Euler method with sampling time $T_s = 0.01[s]$, the discrete-time, state-space system for the pitch subsystem was obtained:

$$\boldsymbol{A}_p = \begin{bmatrix} 1.0000 & 0.0100 \\ -1.2343 & 0.8667 \end{bmatrix}, \tag{38}$$

$$\boldsymbol{B}_p = \begin{bmatrix} 0 \\ 1.2343 \end{bmatrix}, \tag{39}$$

$$\boldsymbol{C}_p = \begin{bmatrix} 1 & 0 \end{bmatrix}. \tag{40}$$

Note that, the torsion angle for the drive train and the angular velocity for the pitch subsystem were unmeasurable during experiments.

Moreover, let us consider the following time-varying bias scenarios:

$$\boldsymbol{f}_{s_{dt},k} = 0.02 \cdot \left(\boldsymbol{C}_{dt}\boldsymbol{x}_k \cdot \sin\frac{k}{500} + \boldsymbol{C}_{dt}\boldsymbol{x}_k \cdot \sin\frac{k}{1000} + \boldsymbol{C}_{dt}\boldsymbol{x}_k\right), \tag{41}$$

$$\boldsymbol{f}_{s_p,k} = 0.05 \cdot \left(\boldsymbol{C}_p\boldsymbol{x}_k \cdot \sin\frac{k}{500} + \boldsymbol{C}_p\boldsymbol{x}_k \cdot \sin\frac{k}{1000} + \boldsymbol{C}_p\boldsymbol{x}_k\right), \tag{42}$$

which consist of dynamic sensor biases dependent on the current state. Such scenarios might happen in real system and could cause its incorrect operation. As a consequence, it even might be a reason of a complete failure of the system.

As a result of solving the problem (19), the following gain matrices were obtained:

$$\boldsymbol{K}_{dt} = \begin{bmatrix} 0.5349 & 0.0154 \\ 0.0688 & 0.3338 \\ 0.2735 & 0.0362 \end{bmatrix}, \tag{43}$$

$$\boldsymbol{K}_p = \begin{bmatrix} 0.5839 \\ -3.8104 \end{bmatrix}, \tag{44}$$

along with $\alpha_{dt} = 0.01$ and $\alpha_p = 0.07$, respectively. Figs. 1 and 2 present the evolution of the trace of matrix $\text{diag}(\boldsymbol{P}, \boldsymbol{R})$ for the drive train and pitch subsystem estimators, respectively. Note that the trace is a measure of the size of a robust invariant set, which describes the uncertainty of the estimates [1]. This means that the bigger the trace the smaller the ellipsoid shaping the invariant set. Figs. 3–5 present the

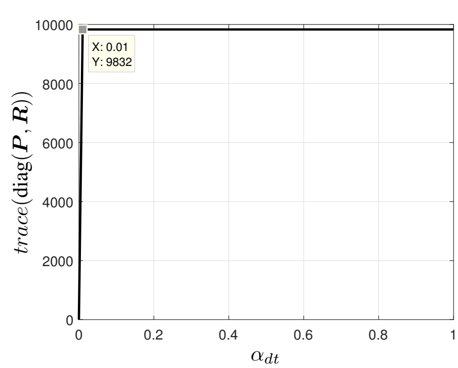

Fig. 1. Evolution of the trace for the drive train

state variables for the ω_r, ω_g and θ_Δ, respectively, which

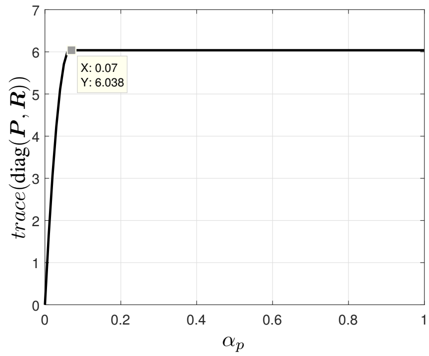

Fig. 2. Evolution of the trace for the pitch subsystem

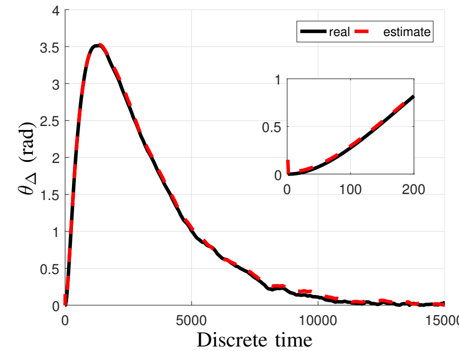

Fig. 5. Drive train torsion angle

are the part of the drive train subsystem. The state estimates are following the real states with a high accuracy in spite of the biased output (depicted by a blue dash-dotted line). Even the state variable θ_Δ, presented in Fig. 5 was unmeasurable, is recovered very well through the robust estimator. Figs.

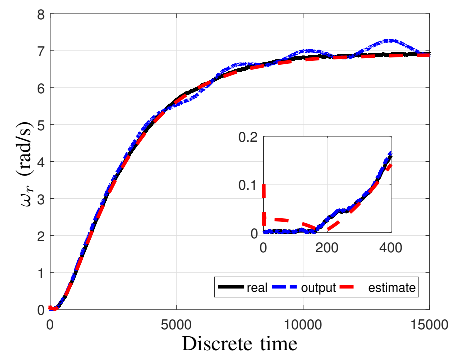

Fig. 3. Drive train rotor speed

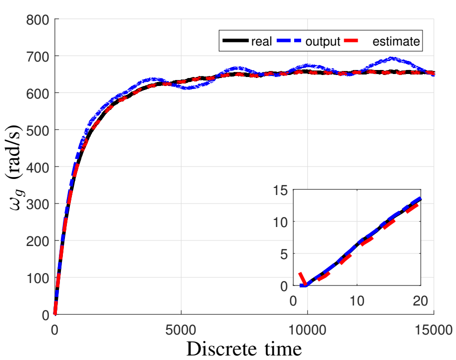

Fig. 4. Drive train generator speed

6–7 present the response of the hydraulic pitch subsystem, namely the state variables for the β_1 and $\dot{\beta}_1$, respectively. Theses plots present responses of the one blade only. In this case, the estimates are pursuing the real states as efficiently as it was for the drive train case despite the biased output. The angular velocity $\dot{\beta}_1$ which was unavailable during the experiments was estimated quite well. The zoomed windows

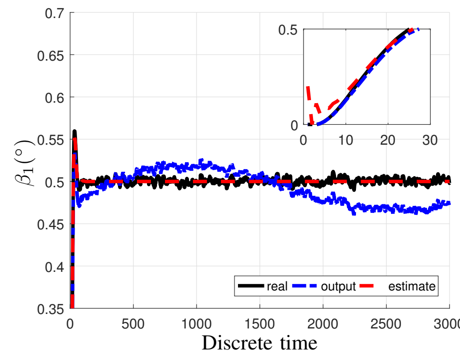

Fig. 6. Pitch angle

of Figs. 3–7 show how fast the state estimate coincide the real state.

A more interesting part of the experiments are the bias estimates. Figs. 8–10 show the real sensor biases as well as their estimates. The estimation error for the rotor speed sensor bias is the biggest one but its magnitude is less than 4% and should be perceived as highly satisfactory one. In the zoomed window of the Fig. 9 a large accuracy of the bias estimate is clearly identified. The estimation error, in this case, is the lowest one and its magnitude varies in about 0.15%. The sensor bias for the pitch angle is portrayed in Fig. 10. The performance of the estimate is quite well and

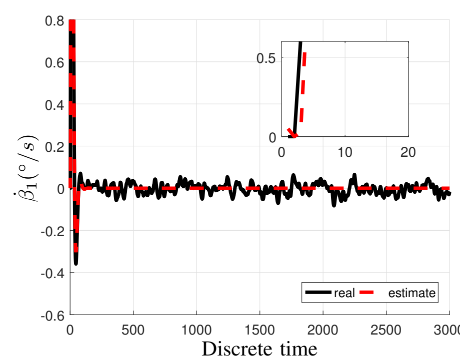

Fig. 7. Angular velocity of the pitch system

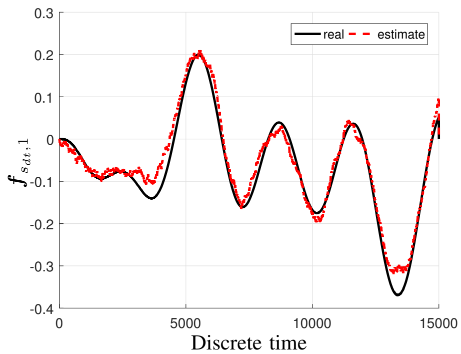

Fig. 8. Rotor speed sensor bias and its estimate

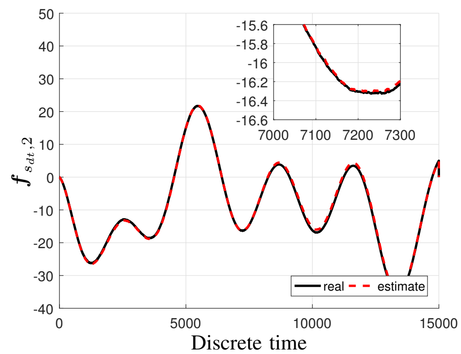

Fig. 9. Generator speed sensor bias and its estimate

the bias estimation error varies up to 3.3%.

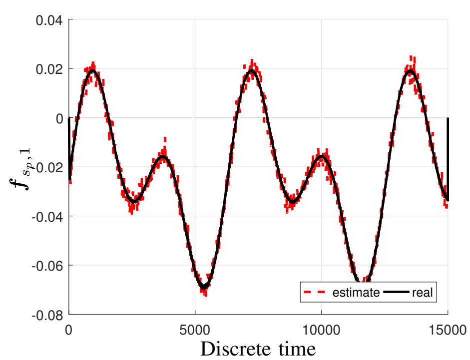

Fig. 10. Pitch angle sensor bias and its estimate

V. CONCLUSIONS

The paper deals with the problem of simultaneous estimation of the state and sensor biases. The developed approach is based on the quadratic boundedness strategy. By few relatively simple transformations of the state-space system, the estimator which was able to estimate the bias-free state of the system was developed. As a result, it was possible to calculate the sensor bias estimate. The advantage of the proposed methodology is its simplicity and it boils down to designing the state estimator. The quadratic boundedness was used to analyse the convergence of the estimator. The final design procedure boils down to solve an LMI. The proposed scheme has been implemented to the well-known wind turbine benchmark model. The achieved results clearly exhibit the efficiency of the proposed methodology and strongly recommend its practical application. The future work will be focused on the extension to simultaneous estimation of sensor and process or/and actuator faults.

REFERENCES

[1] A. Alessandri, M. Baglietto, and G. Battistelli. Design of state estimators for uncertain linear systems using quadratic boundedness. *Automatica*, 42(3):497–502, 2006.

[2] Jovan D Boskovic, S-M Li, and Raman K Mehra. Fault tolerant control of spacecraft in the presence of sensor bias. In *American Control Conference, 2000. Proceedings of the 2000*, volume 2, pages 1205–1209. IEEE, 2000.

[3] EJ Dela Cruz, AT Alouani, TR Rice, and WD Blair. Estimation of sensor bias in multisensor systems. In *Southeastcon'92, Proceedings., IEEE*, pages 210–214. IEEE, 1992.

[4] B Ding. Constrained robust model predictive control via parameter-dependent dynamic output feedback. *Automatica*, 46(9):1517–1523, 2010.

[5] B Ding. Dynamic output feedback predictive control for nonlinear systems represented by a Takagi–Sugeno model. *Fuzzy Systems, IEEE Transactions on*, 19(5):831–843, 2011.

[6] Xiangdong Lin, Y Bar-Shalom, and T Kirubarajan. Exact multisensor dynamic bias estimation with local tracks. *IEEE Transactions on Aerospace and Electronic Systems*, 40(2):576–590, 2004.

[7] Xiangdong Lin, Yaakov Bar-Shalom, and Thiagalingam Kirubarajan. Multisensor multitarget bias estimation for general asynchronous sensors. *IEEE Transactions on Aerospace and Electronic Systems*, 41(3):899–921, 2005.

[8] P. F. Odgaard and K. E. Johnson. Wind turbine fault detection and fault tolerant control - an enhanced benchmark challenge. In *2013 American Control Conference*, pages 4447–4452, June 2013.

[9] P. F. Odgaard, J. Stoustrup, and M. Kinnaert. Fault tolerant control of wind turbines - a benchmark model. In *Proceedings of the 7th IFAC symposium on fault detection, supervision and safety of technical processes (SAFEPROCESS09)*, pages 155–160, 2009.

[10] P. F. Odgaard, J. Stoustrup, and M. Kinnaert. Fault-tolerant control of wind turbines: a benchmark model. *IEEE Transactions on Control Systems Technology*, 21(4):1168–1182, 2013.

[11] Marcin Pazera, Mariusz Buciakowski, and Marcin Witczak. Robust multiple sensor fault-tolerant control for dynamic non-linear systems: application to the aerodynamical twin-rotor system. *International Journal of Applied Mathematics and Computer Science*, 28(2), 2018.

[12] Amir Rafati, Behzad Moshiri, and Javad Rezaei. A new algorithm for general asynchronous sensor bias estimation in multisensor-multitarget systems. In *Information Fusion, 2007 10th International Conference on*, pages 1–8. IEEE, 2007.

[13] Edouard Richard, Mohamed Boutayeb, Hugues Rafaralahy, and Michel Zasadzinski. Design of speed and sensor bias estimator for unmanned aerial vehicle. In *Control Conference (ECC), 2009 European*, pages 701–706. IEEE, 2009.

[14] Lothar Seybold, Marcin Witczak, Paweł Majdzik, and Ralf Stetter. Towards robust predictive fault–tolerant control for a battery assembly system. *International Journal of Applied Mathematics and Computer Science*, 25(4):849–862, 2015.

[15] Arun T Vemuri. Sensor bias fault diagnosis in a class of nonlinear systems. *IEEE Transactions on Automatic Control*, 46(6):949–954, 2001.

[16] William Whitacre and Mark Campbell. Cooperative geolocation and sensor bias estimation for uavs with articulating cameras. In *AIAA Guidance Navigation and Control Conference*, pages 1934–1939, 2009.

[17] Guoguang Zhang, Zitian Yu, and Junmin Wang. Linear parameter-varying observer design for vehicle yaw rate sensor bias estimation and signal reconstruction. In *American Control Conference (ACC), 2016*, pages 2391–2396. IEEE, 2016.

[18] Xiaodong Zhang, Thomas Parisini, and Marios M Polycarpou. Sensor bias fault isolation in a class of nonlinear systems. *IEEE Transactions on Automatic Control*, 50(3):370–376, 2005.